

Impact of isovalent doping on the trapping of vacancy and interstitial related defects in Si

E. N. Sgourou,^{1,a)} D. Timerkaeva,^{2,3,a)} C. A. Londos,¹ D. Aliprantis,¹ A. Chroneos,^{4,5}
 D. Caliste,² and P. Pochet^{2,b)}

¹University of Athens, Solid State Physics Section, Panepistimiopolis Zografos, Athens 157 84, Greece

²Laboratoire de Simulation Atomistique (L_Sim), SP2M, INAC, CEA-UJF, 38054 Grenoble Cedex 9, France

³Kazan Federal University, 18 Kremlevskaya St., Kazan, 420018, Russia

⁴Department of Materials, Imperial College London, London SW7 2AZ, United Kingdom

⁵Materials Engineering, The Open University, Milton Keynes MK7 6AA, United Kingdom

(Received 19 December 2012; accepted 2 March 2013; published online 19 March 2013)

We investigate the impact of isovalent (in particular lead (Pb)) doping on the production and thermal stability of the vacancy-related (VO) and the interstitial-related (C_iO_i and C_iC_s) pairs in 2 MeV electron irradiated Si samples. We compare the Cz-Si samples with high and low carbon concentration, as well as with Pb-C and Ge-C codoped samples. Using Fourier Transform Infrared Spectroscopy (FTIR), we first determine that under the examined conditions the production of VO decreases with the increase of the covalent radius of the prevalent dopant. Moreover, the production of the VO, C_iO_i , and C_iC_s pairs is quite suppressed in Pb-doped Si. In addition, we conclude to an enhanced trapping of both C_i and C_s by Pb impurity under irradiation. The results are further discussed in view of density functional theory calculations. The relative thermodynamic stability of carbon and interstitial related complexes was estimated through the calculations of binding energies of possible defect pairs. This allows to investigate the preferred trapping of vacancies in Pb-doped samples and interstitials in the Ge-doped samples. The different behavior is revealed by considering the analysis of the ratio of vacancy-related to interstitial-related clusters derived from the FTIR measurements. The presence of PbV complexes is confirmed due to the mentioned analysis.

© 2013 American Institute of Physics. [<http://dx.doi.org/10.1063/1.4795510>]

I. INTRODUCTION

Si and its alloys are mainstream materials used in a range of microelectronic and photovoltaic applications. Nevertheless, the understanding of numerous defect-dopant associations, which can affect its properties are still not well established.¹ These can become very important considering that the dimensions of devices are a few nanometers with atomic effects becoming more important. Oxygen (O) and carbon (C) are important impurities in Si, whereas their tendency to associate with intrinsic defects and other impurities leads to numerous clusters that in turn affect the properties of Si.^{2,3}

Infrared spectroscopy (IR) has been used extensively to study the production and annealing behavior of defects in irradiated Si. Localized vibrational modes (LVM) bands from oxygen-related and carbon-related clusters in Si have been identified and attributed to particular structures. It is established that oxygen associates with vacancies and carbon with self-interstitials (I). A band at 830 cm^{-1} has been assigned^{4,5} to the neutral charge state of the VO pairs, which is the main oxygen-related cluster in Si. The main carbon-related pairs are the C_iO_i and the C_iC_s . At least six LVM bands have been assigned³ to the C_iO_i pair, among them the strongest is that at $\sim 860\text{ cm}^{-1}$. For high irradiation fluencies, the C_iO_i pair can associate with self-interstitials and two

bands at 940 cm^{-1} and 1024 cm^{-1} have been correlated with the C_iO_iI cluster.³ The metastable C_iC_s defect gives more rise to more than ten IR band. Five of them have been correlated with the A configuration of the defect and another six IR bands with the B configuration of the defect.⁶ Although the bands are very weak and can be observed only at liquid helium (He) temperatures, a band at 544 cm^{-1} can be detected⁷ at room temperature in carbon-rich Si. Notably, VO, C_iO_i , and C_iC_s pairs introduce deep levels in the energy gap of Si, and therefore, affect its electrical properties. More specifically VO and C_iO_i complexes are thought to act as recombination centers^{8,9} in Si leading to a severe degradation of devices. For C_iC_s , however, recent research on Si lasers has shown¹⁰ that the introduction of this pair can be used to obtain optical gain and stimulated emission that in turn enhance the performance of Si-based devices.

The isovalent doping of Si is an established point defect engineering strategy. In previous studies,^{11–14} we have investigated the effect of Ge doping to radiation harden Si. In particular, it was determined that the production of the VO, C_iO_i , and C_iC_s is generally enhanced¹¹ by the presence of Ge. Additionally, the thermal stability of the VO pair was found to be reduced¹² although that of the C_iO_i and C_iC_s pairs is practically unaffected¹² by Ge. Finally, the percentage of VO defects that are converted to VO_2 defects is reduced¹³ by the presence of Ge.

Considering the case of Pb doping, the picture is less clear. It was determined from electrical measurements^{15,16} that the production of the VO and C_iC_s pairs is suppressed in Pb-doped Si, although there are no related reports about the

^{a)}E. N. Sgourou and D. Timerkaeva contributed equally to this work.

^{b)}Author to whom correspondence should be addressed. Electronic mail: pascal.pochet@cea.fr

C_iO_i pair. Moreover to the best of our knowledge, there are no reports regarding the impact of Pb on the thermal stability of the oxygen-vacancy and carbon-related pairs. Similarly, there are no reports regarding the effect of Pb on the conversion ratio of the VO to the VO_2 defect.

Notably, Pb has a larger covalent radius than that of Si inducing strains in the lattice which can be compensated by the introduction of C, which has a smaller covalent radius than that of Si. In fact, the codoping of Pb and C in Si has been used as a technique to stabilize Pb atoms at substitutional sites and suppress any Pb precipitation.^{15,17} Although there is indirect evidence^{15,16} for the interaction between Pb and C atoms, nevertheless any signal from PbC related complexes has not been detected so far. In general, the introduction of strain fields in the lattice either with the application of external pressure or with the introduction of isovalent impurities with a larger covalent radius can impact the equilibrium concentrations and defect processes (e.g., diffusion) of intrinsic point defects.^{18–20} On the other hand, carbon itself is also an isovalent impurity effectively providing internal local tensile strain to the silicon lattice. Concerning the effect of carbon to the formation of the VO pair, we note that the exact role of carbon is not definitely established so far in the literature. For instance, there are reports stating that VO formation is not affected²¹ by the carbon presence, although other reports have concluded that the carbon presence enhances²² the VO formation.

As it was mentioned above, some species that are present in the samples could remain undetected with an established experimental technique such as IR spectroscopy. This is because the signal from these defects is either too weak or shadowed by other defect complexes. Nevertheless, there is a possibility to investigate thermodynamic and kinetic features of the defects and their complexes on the atomic scale using first principles calculations as recently reviewed in Ref. 23. For instance, this is the case for PbV complex in Pb-doped silicon. PbV complex was predicted to be stable via *ab initio* calculations in a recent paper,²⁰ however, its LVM bands have not been identified so far.

The scope of the present contribution is two-fold. First, we investigate the effect of Pb on the production and the thermal stability of the VO, C_iO_i , and C_iC_s pairs, which allows us to make an assessment of the hardening potential of Pb on these pairs by comparison with the corresponding effect of Ge doping in Si. Second, in order to determine and separate the effect of each dopant on defect formation, we have performed a systematic theoretical study of possible defect pairs. We considered pairs containing C and one of the isovalent impurities (Ge, Sn, Pb) or self-interstitials

which were further studied from a thermodynamic point of view. Such a combined analysis strengthens the possibility to obtain a general picture of the processes in bulk silicon codoped with C and Pb/Ge after irradiation.

II. METHODOLOGY

A. Experimental methodology

We used mainly two groups of Si samples containing carbon, one Ge-doped (labeled CCz-Si:Ge) and the other one Pb-doped (labeled CCz-Si:Pb). The Ge and Pb concentrations were measured by secondary ion mass spectroscopy (SIMS). The oxygen (1106 cm^{-1}) and carbon (606 cm^{-1}) concentrations were calculated using calibration coefficients of $3.14 \times 10^{17}\text{ cm}^{-2}$ and $1.0 \times 10^{17}\text{ cm}^{-2}$, respectively. To compare and to study the influence of carbon on VO pairs production, we used another two groups of Si samples containing relatively high and low carbon doping labeled $C_H\text{Cz-Si}$ and $C_L\text{Cz-Si}$. All the samples were mechanically polished and their thickness was $\sim 2\text{ mm}$. It should be noted that the 606 cm^{-1} band of C_s in the spectra overlaps with some other spectra features. This carbon peak is superimposed in the spectra by the two-phonon absorption band in Si causing difficulties in estimating the exact carbon concentration of the samples. By following a procedure similar to that reported²⁴ previously, we calculated the C_s concentration of the samples. The values cited in Table I are similar to the corresponding values given by the provider with an error of less than 2% for the $C_H\text{Cz-Si}$ sample, 2% for $C_L\text{Cz-Si}$ sample, and $\sim 6\%$ for the CCz-Si:Ge and CCz-Si:Pb samples.

The samples were irradiated with 2 MeV electrons at about $\sim 80^\circ\text{C}$, with a fluence of $1 \times 10^{18}\text{ cm}^{-2}$. Their Ge, Pb, O_i , and C_s concentrations together with other information regarding the radiation-induced defects VO, C_iO_i , C_iC_s , and C_iO_iI are given in Tables I and II. Following the irradiation, all the samples were subjected to 20-min isochronal anneals in open furnaces in $\sim 10^\circ\text{C}$ steps up to about 400°C . After each annealing step, the IR spectra were taken at room temperature by means of a Fourier Transform Infrared (FTIR) spectrometer (JASCO-470Plus) to monitor the thermal evolution of the defects.

B. Theoretical methodology

The BigDFT²⁵ code was used to perform density functional theory (DFT) calculations within Generalized Gradient Approximation (GGA) using the Perdew-Burke-Ernzerhof (PBE) functional.²⁶ This code is using a wavelet basis-set and is very attractive for dealing with complex and

TABLE I. The concentrations of Ge and Pb ([Ge] and [Pb]) and the concentrations of O_i and C_s before irradiation ($[O_i]_o$ and $[C_i]_o$) and after irradiation ($[O_i]_{a.i.}$ and $[C_i]_{a.i.}$).

Sample name	$[O_i]_o\text{ cm}^{-3}$	$[O_i]_{a.i.}\text{ cm}^{-3}$	$[C_s]_o\text{ cm}^{-3}$	$[C_s]_{a.i.}\text{ cm}^{-3}$	[Ge] cm^{-3}	[Pb] cm^{-3}
$C_H\text{Cz-Si}$	9.3×10^{17}	9×10^{17}	22×10^{16}	13.2×10^{16}
$C_L\text{Cz-Si}$	9.5×10^{17}	9.1×10^{17}	5×10^{16}	$< 2 \times 10^{16}$
CCz-Si:Ge	5.2×10^{17}	4.3×10^{17}	4.4×10^{16}	$< 10^{16}$	4×10^{18}	...
CCz-Si:Pb	2.1×10^{17}	1.5×10^{17}	19×10^{16}	$< 10^{16}$	—	1×10^{18}

TABLE II. The production of the VO, C_iO_i and C_iC_s pairs for the various samples. The “ C_iD_s ” column presents the expected but not detectable carbon related defects concentrations $R_{V/I}$ presents the calculated ratio of vacancy-related pairs (VO) to interstitial-related detected clusters (C_iO_i , C_iC_s , C_iO_iI). $R_{V/L_{ext}}$ presents the extended ratio of vacancy-related pairs (VO) with respect to all expected interstitial-related defects.

	$VO \times 10^{16} \text{ cm}^{-3}$	$C_iO_i \times 10^{16} \text{ cm}^{-3}$	$C_iC_s \times 10^{16} \text{ cm}^{-3}$	$C_iO_iI \times 10^{16} \text{ cm}^{-3}$	$C_iD_s \text{ or } C_i \times 10^{16} \text{ cm}^{-3}$	$R_{V/I}$	$R_{V/L_{ext}}$
$C_HCz\text{-Si}$	6.06	5.72	0.036	0.456	0	0.98	0.98
$C_LCz\text{-Si}$	5.8	3	0.02	0.23
$CCz\text{-Si:Ge}$	4.94	2.53	0.029	0.494	0.18	1.62	1.53
$CCz\text{-Si:Pb}$	3.31	1.87	0.016	0.304	8	1.51	0.33

inhomogeneous systems due to the adaptivity of the basis-set. Moreover, the basis-set has high convergence properties and the code can run on massively parallel or hybrid architectures.^{25,27} A simple cubic supercell of 216 atoms was used to construct the defected structures with periodic boundary conditions (PBC). The calculation parameters were chosen in accordance to those reported previously since they have proven to give converged results for vacancy diffusion in similar Si supercells.²⁸ Core electrons were treated within the norm-conserving pseudo-potential approximation using the Hartwigsen-Goedecker-Hutter family.²⁹ The wavelet basis-set accuracy in PBC is given by the grid step size which has been chosen to be 0.4423 Bohr in the three space directions. This value provides variations in formation energies of oxygen related defects in silicon within 20 meV, while the oxygen pseudopotential is harder than all other dopants we introduced (C, Si, Ge, and Pb). Finally, Γ -point alone was used for Brillouin zone integration since the size of the supercell ensures enough convergence for formation and migration energies of defects in silicon.³⁰ For this work, we have calculated the binding energies, E_b , of the defects of interest as $E_b = E_A + E_B - E_{A+B}$ with E_A and E_B being the formation energy of the former isolated defects A and B , and E_{A+B} is the energy of the defect complex. The isolated defect has been calculated in separate Si supercell. Energies already present in references have also been recalculated here for consistency and comparison of obtained results.

III. RESULTS AND DISCUSSION

Figures 1(a)–1(d) show the IR spectra of the $CCz\text{-Si:Ge}$, $CCz\text{-Si:Pb}$, $C_HCz\text{-Si}$, and the $C_LCz\text{-Si}$ samples, respectively, recorded prior and after irradiation. Bands at 830 cm^{-1} (VO), at 862 cm^{-1} (C_iO_i), at 546 cm^{-1} (C_iC_s) as well as the pair of bands at $936, 1020 \text{ cm}^{-1}$ related to the (C_iO_iI) are present as expected in all the samples. Note that the 546 cm^{-1} band is weak and any contribution from the C_iO_i defect was not detected. Figures 2(a)–2(c) present the thermal evolution of the VO, C_iO_i , and C_iC_s pairs, respectively. For the $CCz\text{-Si:Ge}$ sample, the spectral range below 600 cm^{-1} is very noisy and the 546 cm^{-1} band is obscured by this noise. Consequently, the thermal evolution of the band cannot be monitored properly. The band disappears above $\sim 300^\circ \text{C}$ but its decay cannot be followed and therefore it is not presented in Fig. 2(c).

Fig. 2 and the results in Tables I and II represent the production of VO, C_iO_i , C_iC_s , and C_iO_iI pairs in the Pb-doped and Ge-doped Si sample as well as in the samples with high

and low carbon concentration. It is important to note that the initial concentrations of oxygen and carbon are not the same in the samples used. Carbon and oxygen concentrations are expected to affect the introduction rates of the vacancy- and the interstitial-related secondary radiation induced defects. The lower observed concentration of carbon in the Ge-doped sample makes direct comparisons of dopant effect on the VO production difficult as it has been already reported that carbon concentration has a strong effect in Ge-doped samples.¹¹ Nevertheless, we will show that conclusions can be derived from a study of the relative concentration of the various defect clusters made of carbon and vacancy/interstitials. We shall interpret the results depicted in Fig. 2 by mainly exploring the role of isovalent dopants present in the Si lattice. Exploring the obtained IR data, one notices the decrease in production of Frenkel pairs with the increase of the radius of the isovalent dopant. This effect is in line with the oversized dopant-induced Frenkel pair production reduction already proposed previously.²³ To progress further in this analysis, we will now quantify how the produced vacancies and interstitials are trapped with respect to the isovalent impurity.

We start our analysis with the reference sample that contains high concentration of C: $C_HCz\text{-Si}$. The concentrations of the detected oxygen and carbon-related complexes are reported in Table II. Upon irradiation most of the vacancies, that survive annihilation with self-interstitials, are captured by oxygen atoms to form VO pairs. In a first approximation, if one does not take into account that some of the produced vacancies pair together to form divacancies, the concentration of VO defects could be taken as a measure of the vacancies concentration. On the other hand, self-interstitials that survive annihilation with vacancies in the course of irradiation are captured by carbon substitutional atoms converting them to carbon interstitials (C_i). The latter are very mobile at room temperature and interact promptly with O_i and C_s to form C_iO_i , C_iC_s , and C_iO_iI defects. When the oxygen concentration is larger than that of carbon like for the reference sample, the concentration of the C_iO_i defects is dominating and corresponds to more than 90% of the detected interstitial-related defects. By inspection of the results in Table II and particularly the ratio of vacancy related defects to interstitial related defects ($R_{V/I}$), one can immediately see a value of almost 1 indicating that all the created Frenkel pairs had been bound with the oxygen and carbon impurities, respectively, to form the four identified clusters. Such a good balance indicates clearly that indeed all the important vacancy and interstitial-related clusters have been taken into account for the reference $C_HCz\text{-Si}$ sample.

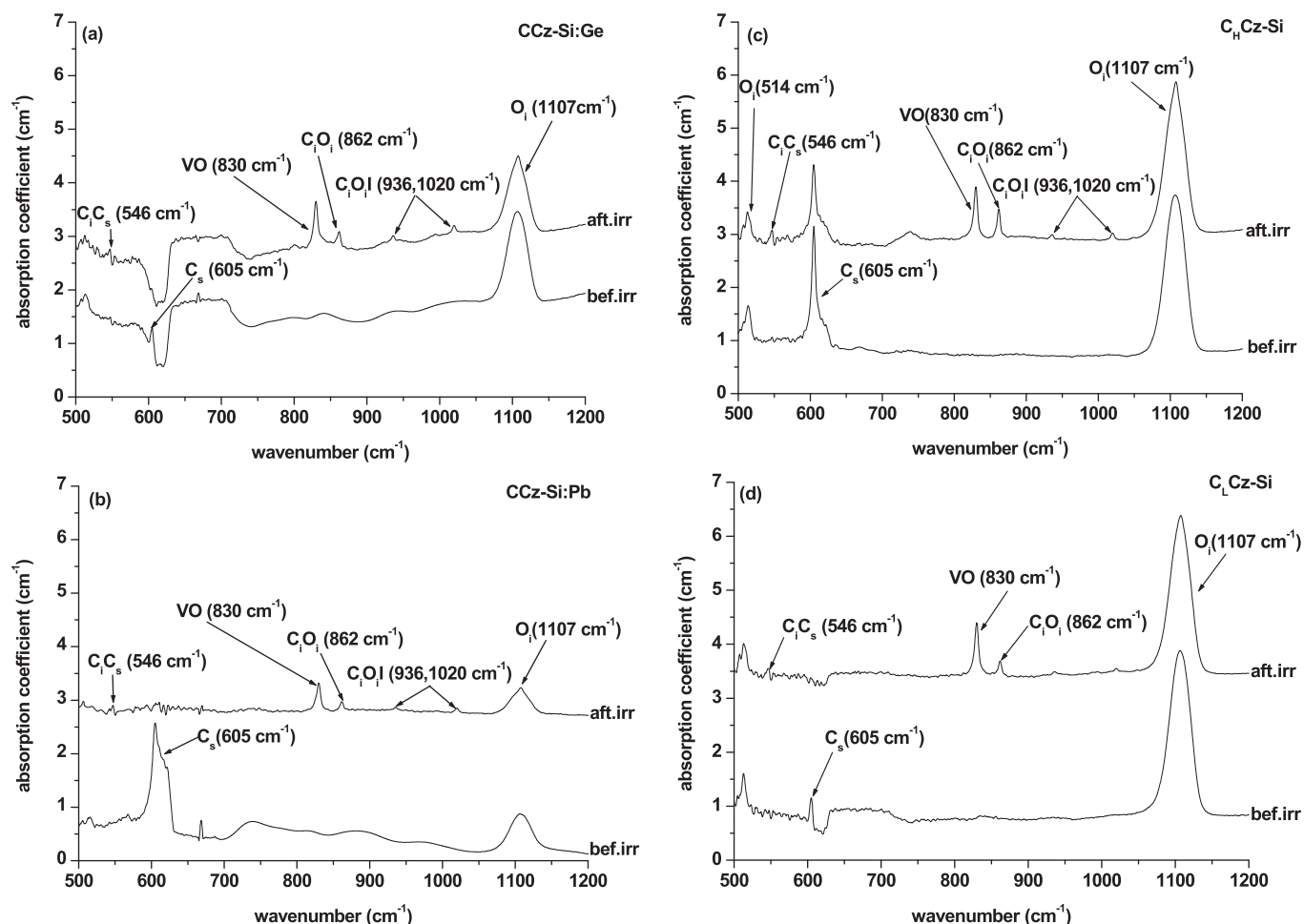


FIG. 1. IR absorption spectra of the (a) CCz-Si:Ge, (b) CCz-Si:Pb, (c) C_H Cz-Si, and (d) C_L Cz-Si samples prior and after electron irradiation.

Regarding now the sample containing low concentration of C: C_L Cz-Si, concentrations of all detected complexes are also presented in Table II. It is likely that all the defect complexes of this high purity sample were detected during the irradiation course. The comparison of the two only with carbon doped samples C_H Cz-Si and C_L Cz-Si allows us to conclude, that doping with lower covalent radius leads to higher VO pairs production under the same irradiation conditions. This point will be further discussed in view of DFT results. In the case of the Ge and Pb-doped samples, the concentration of the C_iO_i defects is substantially lower than that of the VO defects (see Table II) suggesting that isovalent dopants play a key role in the reduction of the detected defect clusters. Interestingly, the $R_{V/I}$ is over-balanced for both Ge and Pb. This result is puzzling as it indicates the same kind of behavior for both samples, although dopant interactions with vacancies and interstitials are different. Since some vacancy- and interstitial-related defects might not be detected by FTIR it seems reasonable to consider theoretical calculations in order to identify possible missing complexes.

To begin with, we consider vacancy-related defects in Ge and Pb doped samples. Both Ge and Pb are isovalent impurities in Si with a covalent radius larger than that of Si. Therefore, both these oversized isovalent dopants introduce local strains in the Si lattice, which can be relieved by the association with vacancies. For Ge-doped Si, the formation of

the GeV pair has been previously reported^{31,32} in low temperature irradiated Si. GeV is stable up to about 200 K and then dissociates effectively liberating the trapped V. Although it is expected theoretically, the formation of PbV pairs has not been observed experimentally yet.²³ The thermodynamic stability of defect clusters can be estimated through their binding energies. The lower is the value of the binding energy the stronger is the association between the defects. The corresponding binding energies of the VO and GeV pairs are found to be 1.53 eV and 0.27 eV, respectively. These values are consistent with previous results^{30,33} indicating that when an O and a Ge compete for a V the formation of the VO pair will be prevalent. For Pb-doped Si, the tendency of Pb to associate with vacancies is larger than that of Ge, due to its considerable higher covalent radius, leading to a larger reduction of VO pairs. Indeed, previous DFT calculations indicate that the PbV pair has a binding energy of 1.37 eV.²³ This implies that Pb will compete more effectively for the available V than Ge and, therefore, it will have a more significant impact on the reduction of the concentration of VO pairs.

The situation is less clear in the case of interstitial-related defects. To further clarify this point, we have calculated using DFT the binding energy of possible defects including carbon and/or dopant and/or interstitial silicon, the dopant being an element of the IVth column (C, Ge, Sn, Pb). Three types have been considered in the following: (i) the carbon substitutional/

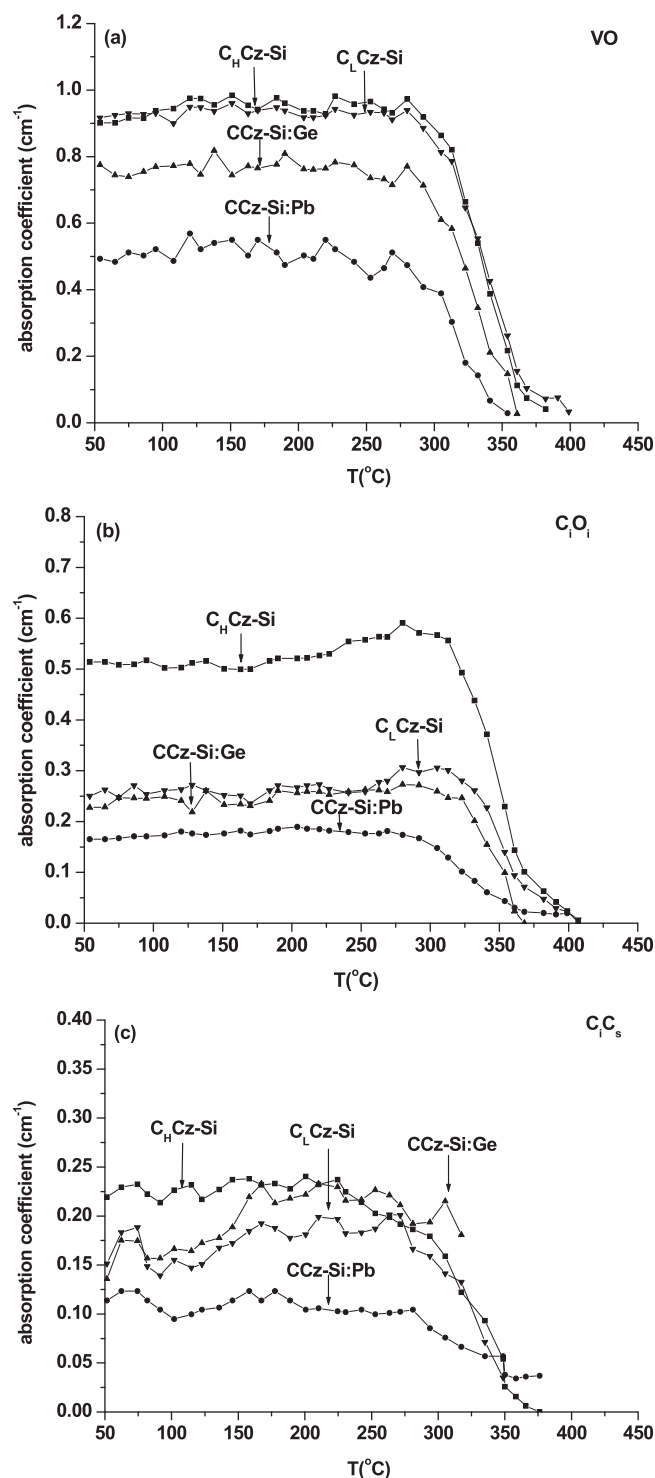


FIG. 2. The production of the (a) VO, (b) $C_i O_i$, and (c) $C_i C_s$ pairs for the $C_H Cz-Si$, $C_L Cz-Si$, $CCz-Si:Ge$, and $CCz-Si:Pb$ samples.

dopant substitutional complex $C_s D_s$, (ii) the carbon interstitial/dopant substitutional complex $C_i D_s$, and (iii) the dopant substitutional/silicon interstitial complex $D_s I$.

For the $C_s D_s$ pairs, the binding energy has been calculated up to the fourth nearest neighbour (Fig. 3). From this, we first can claim that $C_s C_s$ pair is unlikely to form in isovalent doped silicon samples as the binding energy is always negative and as low as -1.5 eV for the first neighboring C_s . For the $C_s Ge_s$ pair, the binding energy is always close to

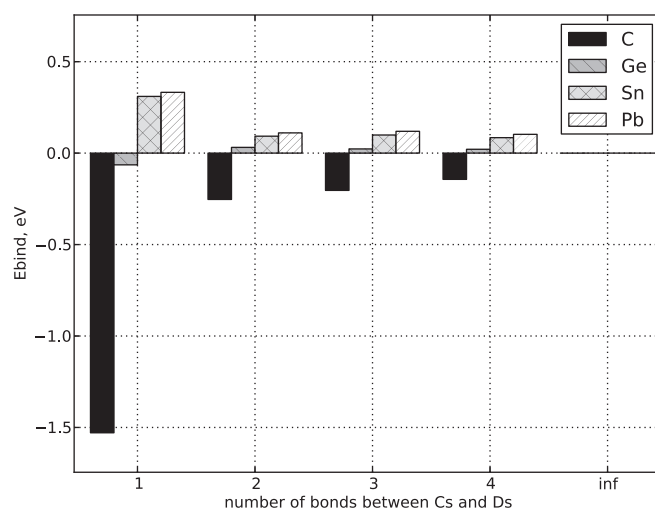


FIG. 3. Binding energies for $C_s D_s$ complexes depending on the distance between the components of the defect. The $C_s C_s$ defect was found to be unfavored, whereas Pb and Sn form the stable complexes with carbon as a first neighbour with the formation energy around 0.3 eV. The $Ge_s C_s$ complex is shown to have a binding energy close to zero.

zero. However, Pb and Sn represent positive binding energies with a maximum absolute value of about 0.3 eV when Pb_s and Sn_s are the first neighbors of a C_s .

For the $C_i D_s$ pair, the binding energy has been calculated only when the interstitial is first neighbor of the D_s . The choice of reference is not straightforward as the most stable orientation of the interstitial Si and over-sized impurities is the $\langle 110 \rangle$ configuration while it is the $\langle 100 \rangle$ for carbon. Notably, the choice of the reference will only change the absolute value of the series but not the difference between the four impurities. Using the $\langle 100 \rangle$ silicon interstitial as a reference, we found a binding energy of 1.34 eV for the $C_i C_s$ (see Fig. 4). This strong binding energy is in the line with the formation of such a complex in our samples. For $C_i Ge_s$, the resulting binding energy is found to be 0.46 eV. And as for the $C_i D_s$ complex, Pb and Sn have the same behavior and a positive binding energy of 0.3 eV.

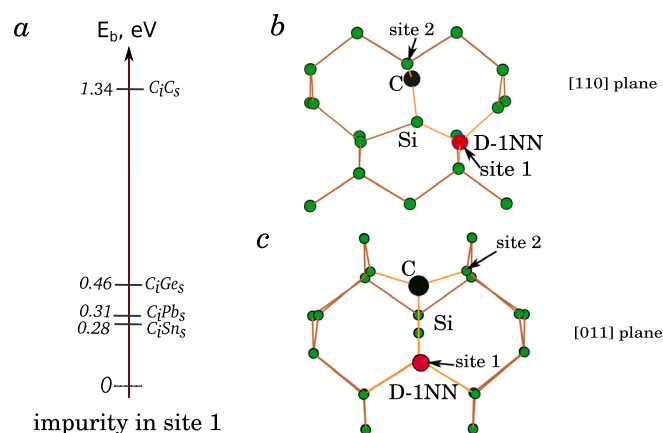


FIG. 4. (a) Binding energies for $C_i D_s$ complexes. $C_i C_s$ is the most stable configuration with binding energy of 1.34 eV (b) ID_s defect scheme, front view (c) ID_s defect scheme, side view. The site 2 is another possible position of D_s as the first nearest neighbor of C_i , but these configurations are less stable for all the tested elements.

For the D_sI pair, the binding energy has been calculated also only for the first nearest neighbor configurations. Taking as a reference the $\langle 110 \rangle$ silicon interstitial, the binding energy for the D_sI pairs is found to be close to zero or slightly negative for all studied complexes except C_sI that is bound by 0.87 eV. This pair is expected to further transform to C_i with an energy gain of 1.44 eV. This energy will be called from now on as the binding energy of C_i , corresponding to the association from separated C_s and I . The geometries of these two defects are represented in Figs. 5(a) and 5(b). The reconstruction could be performed through the carbon migration as indicated by arrows on Fig. 5(a) (not calculated). However, as the theoretical study of kinetic properties is out of the scope of the present study, the corresponding migration barriers have not been calculated. From the above DFT results, it is clear that C_s is the strongest trap for self-interstitials. This is in agreement with previous experimental findings on this issue³ and references therein.

The positive binding energies of the defect clusters are listed in Table III. In order to estimate the value of the minimal binding energy to form the stable defect at irradiation temperature of 80 °C, the mass action law can be considered. For large binding energies $E_b > 0.3$ eV, the complex formation is controlled entirely by the pairing kinetics that is out of the scope of present study. Therefore, we will consider these complexes as favorable ones. For E_b smaller than

TABLE III. The calculated binding energies of the most stable defect complexes.

Complex	E _b , eV
C_sPb_s	0.33
C_iC_s	1.34
C_iGe_s	0.46
C_iPb_s	0.31
C_sI	0.87
Dumb bell C_i	1.44
PbV	1.37
GeV	0.27

0.3 eV the dissociation, and hence a precise value of E_b , is essential. This is the case for GeV defect pairs in Table III. This defect cannot be formed at all at 80 °C due to the low equilibrium ratios of GeV and V . Consequently, this complex may be considered as transient during the irradiation flow. Based on these precepts, the following analysis of defect clustering has been performed.

From the values presented in Table III, it is evident that C_s tends to interact with I as well as with C_i . Regarding the effect of carbon doping on the VO production, high carbon contamination can affect VO production rate through the capturing of self-interstitials and preserving them from annihilation with vacancies during the irradiation flow. This is also supported with experiment as the detected VO concentration in a low carbon doped sample is reduced in comparison with the reference sample with high carbon concentration (Table II).

One can compare the binding energies of Table III, which correspond to clusters containing the same dopant. If one compares the clusters containing Pb , it can be seen that Pb forms complexes with vacancies. On the contrary, the Ge atom binds with interstitial carbon with the energy gain of 0.46 eV.

To investigate further the possible clustering within our codoped samples, we analyze the carbon distribution before and after irradiation. The data are reported in Table IV. In the case of the C_HCz-Si and the Ge -doped sample, the situation is rather clear as about 90% of the initial substitutional carbon is dispatched between substitutional carbon and the three carbon interstitial related clusters. But for the Pb -doped sample, only 16.9% of the initial substitutional carbon is detected after irradiation. Following our DFT results summarized in Table III, we can infer that the missing carbon can be distributed between C_iPb_s , C_sPb_s , and C_i defects which are undetected clusters. The concentration of the lost carbon matches a value as high as $16 \times 10^{16} \text{ cm}^{-3}$, thus changing drastically the balance of the $R_{V/I}$. As an example, if we consider half of the missing carbon atoms to be involved in the undetected interstitial-related clusters, C_iPb_s or dumbbell C_i , the resulting extended value of ratio of vacancy- to interstitial-related defects ($R_{V/I_{ext}}$) reduces from the measured value of 1.51 to a suggested value of 0.33. The same analysis applied in the case of the Ge -doped sample only changes slightly the $R_{V/I_{ext}}$ from measured 1.62 down to 1.53 (Table II).

The opposite behavior in the balance of $R_{V/I_{ext}}$ between Ge and Pb doped samples is consistent with their DFT-derived binding energies. Indeed, for the dopant- V pairs, there is a

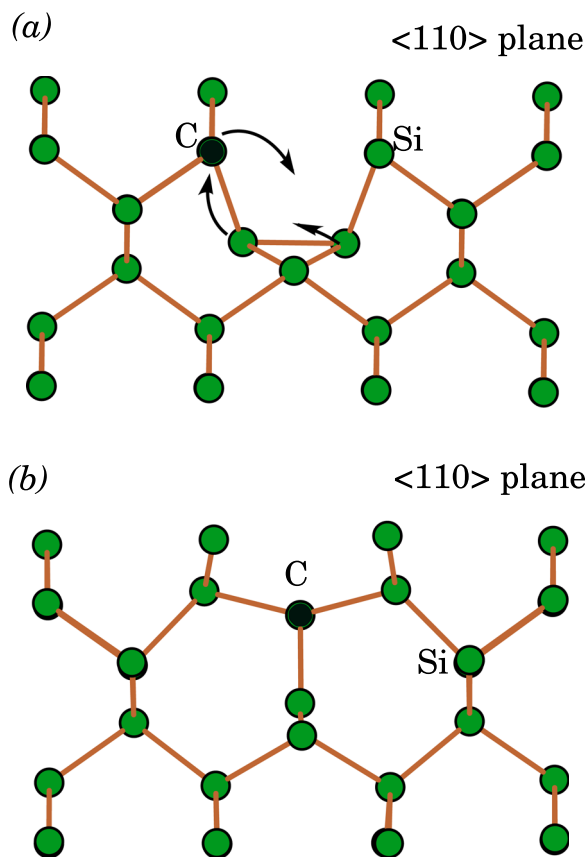


FIG. 5. The configuration schemes of (a) C_sI and (b) C_i defects. C_sI is C_s combined with $\langle 110 \rangle$ split self-interstitial and C_i is $\langle 100 \rangle$ split mixed C-Si interstitial. The probable reconfiguration path from C_sI to C_i is denoted with arrows on (a).

TABLE IV. Carbon related defects before and after irradiation.

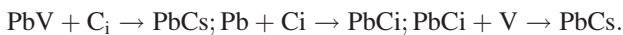
	$C_{s,0} \times 10^{16} \text{ cm}^{-3}$	$C_i O_i \times 10^{16} \text{ cm}^{-3}$	$C_i C_s \times 10^{16} \text{ cm}^{-3}$	$C_i O_i I \times 10^{16} \text{ cm}^{-3}$	$C_s \times 10^{16} \text{ cm}^{-3}$	$\sum C_{\text{aft}} \times 10^{16} \text{ cm}^{-3}$	$C_{s,0} - \sum C_{\text{aft}} \times 10^{16} \text{ cm}^{-3}$
$C_H C_z$ -Si	22	5.72	0.036	0.456	13.2	19.45	2.6 (11.6%)
CC_z -Si:Ge	4.4	2.53	0.029	0.494	1	4.08	0.3 (7.3%)
CC_z -Si:Pb	19	1.87	0.016	0.304	1	3.21	15.8 (83.1%)

stronger binding energy for the PbV than the GeV pairs. Moreover, the DFT calculations have illustrated that the situation is opposite in the case of interstitial related defects as the binding energy of the interstitial with a Ge atom is stronger than that with a Pb atom.

Importantly, the unbalance of $R_{V/I_{\text{ext}}}$ clearly indicates that either vacancy- (for $R_{V/I_{\text{ext}}} < 1$) or interstitial-related (for $R_{V/I_{\text{ext}}} > 1$) defects are missing in the FTIR analysis. In other words, vacancy-related defects in the case of Pb-doped and interstitial-related in the case of Ge-doped are trapped by the corresponding impurity in the sample.

Taking into account that the binding of PbV is very stable, we can assume that the current observation of vacancy loss is an experimental evidence of the PbV presence in Pb doped sample.

In other words, our theoretical results allow us to claim, that Pb and C codoping of crystalline silicon leads to the reduction of VO pairs due to the trapping of V by Pb during the irradiation with high energy electrons. On the other hand, Pb can trap both C_s and C_i species in order to form complexes during the course of irradiation as revealed by the positive binding energies of $C_s Pb_s$ and $C_i Pb_s$ pairs of 0.33 eV and 0.31 eV, respectively. Such behavior would explain the experimentally reported carbon leakage. As vacancies and carbon interstitials are the fast diffusing species, these complexes can be formed by following reactions:



Notably, the balance between vacancies and interstitials is a very informative tool to study defect complexes formation in irradiated material. Moreover, the balance of the impurity species before and after irradiation is an important indicator of the processes that occurred. Such kind of balance analysis together with calculations from the first principles allows to investigate the complex behavior of defects and impurities as well as their fundamental properties in the material.

According to the theoretical and experimental results, it is evident that the role of isovalent dopants on the production of vacancy- and interstitial-related defect complexes is of high

importance. In addition, each dopant interacts with vacancies and interstitial in its own way depending on its covalent radius. The relative strength of such interactions is derived from DFT and presented in Table V. It can be concluded that the smaller the covalent radius is, the higher is the binding energy with interstitials and vice versa vacancies bind stronger with higher covalent radius dopants. Of special interest is the Ge doped case where we have medium values for both I and V. Such a case would be very sensitive to the dopant concentrations as it was shown previously in Ref. 11. Other elements show more straightforward tendencies. C doping will lead to the increase of VO complexes due to the trapping of interstitials by carbon impurities. Whereas in Pb and Sn doping case, the concentration of VO pairs should decrease due to the trapping of some vacancies by dopant elements. The situation becomes more complicated in the codoped case, when relative concentration and interactions between codopants play a crucial role.

The discussion above concerns the thermodynamic aspects of the problem. Further, we will briefly consider the kinetic features of the examined complexes. Previously, we argued that the absence of an inverse annealing stage of the VO in the Pb doped sample indicates the PbV stability above the temperature where VO pairs begin to transform to VO_2 (300 °C).³⁴ Indeed the absence of an inverse annealing stage indicates that this complex is stable in the whole observed temperature range. Moreover, this could explain the increasing of the VO_2 clusters at 450 °C as was reported recently.³⁵ This might happen due to the dissociation of PbV and further reaction with free V with O_2 ($V + O_2 \rightarrow VO_2$).

IV. CONCLUSIONS

The present results verify that the formation of the VO, the $C_i O_i$, and the $C_i C_s$ pairs is substantially reduced in the Pb-doped Si as compared to the reference sample. Regarding the thermal evolution of the above pairs, their annealing temperature is clearly lower in the case of the Pb-doped Si. To conclude, Pb doping can be used to improve the radiation hardness of Si. The different behaviour is revealed by analysis of the ratio of vacancy-related to interstitial-related defects derived from the FTIR measurements. The vacancy trapping by the lead impurity is a further evidence of the presence of the inferred PbV pair.²³ The interstitial trapping by Ge dopants is in line with the proposed mechanism of interstitial release in such Ge-doped samples.^{12,35} Concerning carbon, our DFT calculations prove that it is the strongest trap for the interstitials leading to an increase of the VO concentration with the increase of C concentration. Moreover, we observe an enhanced-capture of both C_i and C_s by Pb impurity under irradiation.

TABLE V. Relative trapping forces of I and V by isovalent dopants (C, Ge, Sn, and Pb) and O. «-» indicates unstable complexes, «+» indicates stable ones.

	C	Ge	Sn	Pb	O
V	-	++	+++	++++	++++
I	++++	++	-	-	-

ACKNOWLEDGMENTS

This work was partially funded by the French National Research Agency through the BOLID Project ANR-10-HABISOL-001. Calculation time was provided by the French GENCI Agency under Project No. t2011096107.

- ¹S. Takeuchi, Y. Shimura, O. Nakatsuka, S. Zaima, M. Ogawa, and A. Sakai, *Appl. Phys. Lett.* **92**, 231916 (2008); E. Kamiyama, K. Sueoka, and J. Vanhellemont, *J. Appl. Phys.* **111**, 083507 (2012); A. Chroneos, R. W. Grimes, and H. Bracht, *J. Appl. Phys.* **105**, 016102 (2009); A. Chroneos, C. A. Londos, and E. N. Sgourou, *J. Appl. Phys.* **110**, 093507 (2011); D. Caliste and P. Pochet, *Phys. Rev. Lett.* **97**, 135901 (2006).
- ²R. C. Newman and R. Jones, "Oxygen in silicon," in *Semiconductors and Semimetals*, edited by F. Shimura, (Academic Press, Orlando, 1994), Vol. 42, p. 289.
- ³G. Davies and R. C. Newman, in *Handbook of Semiconductors*, edited by S. Mahajan (Elsevier, Amsterdam, 1994), Vol. 3, p. 1557–1635.
- ⁴J. W. Corbett, G. D. Watkins, and R. S. McDonald, *Phys. Rev.* **135**, A1381 (1964).
- ⁵C. A. Londos, L. G. Fytros, and G. J. Georgiou, *Defect Diffus. Forum* **171–172**, 1 (1999).
- ⁶E. V. Lavrov, L. Hoffmann, and B. B. Nielsen, *Phys. Rev. B* **60**, 8081 (1999).
- ⁷C. A. Londos, M. S. Potsidi, and E. Stakakis, *Physica B* **340–342**, 551 (2003).
- ⁸S. D. Brotherton and P. Bradley, *J. Appl. Phys.* **53**, 5720 (1982).
- ⁹A. Khan, M. Yamaguchi, Y. Ohshita, N. Dharmarasu, K. Araki, T. Abe, H. Itoh, T. Ohshima, M. Imaizumi, and S. Matsuda, *J. Appl. Phys.* **90**, 1170 (2001).
- ¹⁰K. Murata, Y. Yasutake, K. Nittoh, S. Fukatsu, and K. Miki, *AIP Adv.* **1**, 032125 (2011).
- ¹¹C. A. Londos, A. Andrianakis, V. Emtsev, and H. Ohyama, *Semicond. Sci. Technol.* **24**, 075002 (2009).
- ¹²C. A. Londos, A. Andrianakis, E. N. Sgourou, V. Emtsev, and H. Ohyama, *J. Appl. Phys.* **107**, 093520 (2010).
- ¹³C. A. Londos, A. Andrianakis, E. N. Sgourou, V. Emtsev, and H. Ohyama, *J. Appl. Phys.* **109**, 033508 (2011).
- ¹⁴C. A. Londos, A. Andrianakis, V. Emtsev, and H. Ohyama, *J. Appl. Phys.* **105**, 123508 (2009).
- ¹⁵M. L. David, E. Simoen, C. Clays, V. B. Neimash, M. Kra'sko, A. Kraitichinskii, V. Voytovych, A. Kabaldin, and J. F. Barbot, *J. Phys.: Condens. Matter* **17**, S2255 (2005).
- ¹⁶V. B. Neimash, V. V. Voytovych, M. M. Kra'sko, A. M. Kraitichinskii, O. M. Kabaldin, Yu. V. Pavlov's'kyi, and V. M. Tssmots, *Ukr. J. Phys.* **50**, 1273 (2005), <http://ujp.bitp.kiev.ua/files/journals/50/11/501110p.pdf>.
- ¹⁷K. Milants, J. Verheyden, T. Balancira, W. Deweerdt, H. Pattyn, S. Bukshpan, D. L. Williamson, F. Vermeiren, G. Van Tendeloo, C. Vieken, S. Libbrecht, and C. Van Haesendonck, *J. Appl. Phys.* **81**, 2148 (1997).
- ¹⁸V. V. Emtsev, Jr., C. A. J. Ammerlaan, V. V. Emtsev, G. A. Oganessian, B. A. Andreev, D. F. Kuritsyn, A. Misiuk, B. Surma, and C. A. Londos, *Phys. Status Solidi B* **235**, 75 (2003); A. Misiuk, J. Bak-Misiuk, A. Barcz, A. Romano-Rodriguez, I. V. Antonova, V. P. Popov, C. A. Londos, and J. Jun, *Int. J. Hydrogen Energy* **26**, 483 (2001).
- ¹⁹K. Z. Rushchanskii, P. Pochet, and F. Lançon, *Appl. Phys. Lett.* **92**, 152110 (2008); D. Caliste, K. Rushchanskii, and P. Pochet, *Appl. Phys. Lett.* **98**, 031908 (2011).
- ²⁰A. Chroneos, C. A. Londos, E. N. Sgourou, and P. Pochet, *Appl. Phys. Lett.* **99**, 241901 (2011).
- ²¹A. Bean, R. C. Newman, and R. S. Smith, *J. Phys. Chem. Solids* **31**, 739 (1970).
- ²²V. D. Akhmetov and V. V. Bolotov, *Radiat. Eff.* **52**, 149 (1980).
- ²³P. Pochet and D. Caliste, *Mater. Sci. Semicond. Process.* **15**, 675 (2012).
- ²⁴C. A. Londos, G. D. Antonaras, M. S. Potsidi, D. N. Aliprantis, and A. Misiuk, *J. Mater. Sci.: Mater. Electron.* **18**, 721 (2007).
- ²⁵L. Genovese, A. Neelov, S. Goedecker, T. Deutsch, S. A. Ghasemi, A. Willand, D. Caliste, O. Zilberberg, M. Rayson, A. Bergman, and R. Schneider, *J. Chem. Phys.* **129**, 014109 (2008).
- ²⁶J. P. Perdew, K. Burke, and M. Ernzerhof, *Phys. Rev. Lett.* **77**, 3865 (1996).
- ²⁷L. Genovese, M. Ospici, T. Deutsch, J. F. Mehaut, A. Neelov, and S. Goedecker, *J. Chem. Phys.* **131**, 034103 (2009).
- ²⁸E. Machado-Charry, L. K. Beland, D. Caliste, L. Genovese, T. Deutsch, N. Mousseau, and P. Pochet, *J. Chem. Phys.* **135**, 034102 (2011).
- ²⁹M. Krack, *Theor. Chem. Acc.* **114**, 145 (2005).
- ³⁰D. Caliste, P. Pochet, T. Deutsch, and F. Lançon, *Phys. Rev. B* **75**, 125203 (2007).
- ³¹A. Brelot and J. Charlemagne, in *Radiation Effects in Semiconductors*, edited by J. W. Corbett and G. D. Watkins (Gordon and Breach, New York, 1971), p. 161.
- ³²A. Brelot, in *Radiation Damage and Defects in Semiconductors*, edited by J. E. Whitehouse (Institute of Physics, London, 1973), p. 191.
- ³³A. Chroneos and C. A. Londos, *J. Appl. Phys.* **107**, 093518 (2010).
- ³⁴C. A. Londos, D. Aliprantis, E. N. Sgourou, A. Chroneos, and P. Pochet, *J. Appl. Phys.* **111**, 123508 (2012).
- ³⁵V. V. Voronkov, R. Falster, C. A. Londos, E. N. Sgourou, A. Andrianakis, and H. Ohyama, *J. Appl. Phys.* **110**, 093510 (2011).